Gelation, clustering, and crowding in the electrical double layer of ionic liquids

Zachary A. H. Goodwin, Michael McEldrew, J. Pedro de Souza, et al.

View Online **Export Citation** **CrossMark**

ARTICLES YOU MAY BE INTERESTED IN

Gelation, clustering, and crowding in the electrical double layer of ionic liquids

View Online   Export Citation   CrossMark

Zachary A. H. Goodwin,[1,2,a)] (iD) Michael McEldrew,[3] J. Pedro de Souza,[3] (iD) Martin Z. Bazant,[3,4,b)]
and Alexei A. Kornyshev[1,2,5,c)] (iD)

AFFILIATIONS

[1] Department of Chemistry, Imperial College of London, Molecular Sciences Research Hub, White City Campus, Wood Lane, London W12 0BZ, United Kingdom
[2] Thomas Young Centre for Theory and Simulation of Materials, Imperial College of London, South Kensington Campus, London SW7 2AZ, United Kingdom
[3] Department of Chemical Engineering, Massachusetts Institute of Technology, Cambridge, Massachusetts 02142, USA
[4] Department of Mathematics, Massachusetts Institute of Technology, Cambridge, Massachusetts 02142, USA
[5] Institute of Molecular Science and Engineering, Imperial College of London, South Kensington Campus, London SW7 2AZ, United Kingdom

[a)] Author to whom correspondence should be addressed: zachary.goodwin13@imperial.ac.uk
[b)] bazant@mit.edu
[c)] a.kornyshev@imperial.ac.uk

ABSTRACT

Understanding the bulk and interfacial properties of super-concentrated electrolytes, such as ionic liquids (ILs), has attracted significant attention lately for their promising applications in supercapacitors and batteries. Recently, McEldrew *et al.* [J. Phys. Chem. B **125**, 2677 (2021)] developed a theory for reversible ion associations in bulk ILs, which accounted for the formation of all possible (Cayley tree) clusters and a percolating ionic network (gel). Here, we adopt and develop this approach to understand the associations of ILs in the electrical double layer at electrified interfaces. With increasing charge of the electrode, the theory predicts a transition from a regime dominated by a gelled or clustered state to a crowding regime dominated by free ions. This transition from gelation to crowding is conceptually similar to the overscreening to crowding transition.

I. INTRODUCTION

Ionic liquids (ILs) are concentrated electrolytes solely composed of molecular ions, which are often bulky and asymmetric.[1–4] As such, an IL does not contain electrolyzable solvents, and therefore, the electrochemical stability window of ILs is typically larger than that of dilute aqueous electrolytes.[3] This property permits larger voltages for operation in supercapacitors, which increases the energy that can be stored in the device.[5,6] The promise of IL-based technologies has caused significant interest in understanding ILs and other concentrated electrolytes, such as water-in-salt electrolytes (WiSEs)[7–17] and salt-in-ILs (SiILs).[18–24]

Indeed, owing to the high concentration and lack of high dielectric solvent, the energy of electrostatic interactions between nearest

neighbors is much larger than thermal energy.[3] This manifests through decaying oscillations in charge density around an ion in the bulk or as a function of distance from an interface,[25–27] referred to as overscreening,[28] which can give long-ranged electrostatic screening lengths.[29–33] It was shown by Levy *et al.*[34] that these overscreening structures, from molecular dynamics simulations, can be well described by a nearest-neighbor spin-glass model, which suggests these long-ranged structures are built upon short-ranged Coulomb interactions.

Surprisingly, surface force measurements performed in ILs have reported extremely long-ranged *monotonic* decay lengths,[35–44] referred to as underscreening.[45,46] Gebbie *et al.*[36,37] interpreted these results as ILs behaving as "dilute electrolytes," with ≪1% of ions free and the remaining ions being bound in neutral ion pairs, which do

not participate in electrode screening. Whereas, Han *et al.*[40] have proposed that these long-ranged screening lengths arise because of the ~10 nm domain formation of nano-aggregates in ILs, with indications of these large aggregates being observed in molecular simulations.[47–50]

These observations motivated many to study the role of ion pair formation in ILs,[51–57] and Avni *et al.*[58] even accounted for small finite aggregates (triples and quadruplets). Sometimes, only free ions were explicitly treated, with ion pairs being implicitly treated as "voids."[59–62] This proved to be successful in reproducing the conductivity of ILs based on a Nernst–Einstein relation,[62] where 10%–20% of ions were free, with the remaining being bound up in immobile aggregates. A dynamic exchange between these two states occurs, with a small activation energy ($\sim 1 \ k_B T$) for the excitation from "bound" state to the "free" state. Thus, the concept of an intrinsic narrow gap "ionic semiconductor," as introduced in Ref. 3, has received substantiation.[62] That work showed a dynamic picture of the free ions, but the exact nature of the immobile clusters was not discerned. Moreover, free ion approaches were also able to explain the qualitative changes in differential capacitance as a function of temperature,[60] where a "melting" of "frozen" structures is observed to occur as a function of increasing temperature and voltage. However, the fraction of free ions there was inferred from fitting the differential capacitance, and the nature of the "frozen" states was only discussed on a qualitative level.

There is no doubt that in such a concentrated system as ILs, the formation of clusters larger than ion pairs should occur.[47,48,50,63] McEldrew *et al.*[49,64–66] developed a theory, based on the theories of thermoreversible polymers,[67–75] which was able to systematically describe clusters beyond ion pairs, and even a percolating ionic network of infinite size,[76–78] referred to as the gel. One of the main parameters of the theory is the number of associations an ion can make, where it is assumed cations can only bond to anions and vice versa, which determines the possible clusters that can be formed. If ions can only form one bond, then ion pairs can only occur. If a cation has four association sites, it can form various clusters; for clusters containing a single cation, there can be free cations, neutral ion pairs, and negatively charged triples, quadruplets and quintuplets, as schematically shown in Fig. 1. These clusters can be much larger if more cations are involved, which are accounted for in the theory of McEldrew *et al.*[49,64–66]

The theory of McEldrew *et al.*[64] was applied to bulk ILs,[49] where a consistent theory of ionic transport was also developed based on vehicular motion of the clusters,[49,79] and other concentrated electrolytes.[65,66] While the ionic association theory has given a detailed description of the cluster statistics in the bulk, it has not yet been applied to predict the distributions of clusters near charged interfaces in the electrical double layer (EDL).[80]

Here, we develop a theory of aggregation and gelation of ILs in the EDL. Before proceeding to the mathematical formalism of this theory, we briefly discuss the principles of the chemical equilibrium that hold in a theory accounting for thermoreversible associations in the bulk and the EDL of ILs. This discussion will be followed by a short preview of the results, which shall foreshadow the remaining paper.
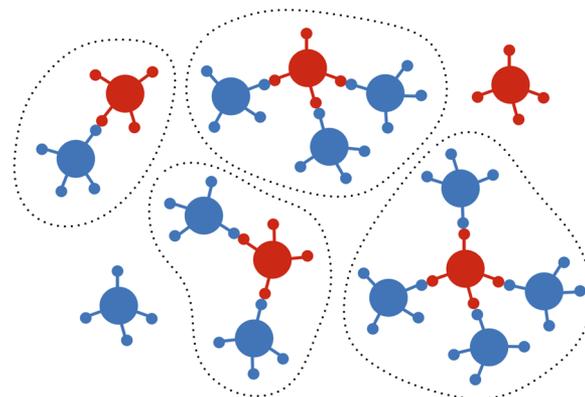

FIG. 1. Schematic of possible aggregates containing one cation. Cations are shown in red and anions in blue, where both can form a maximum of four associations, as shown by the "dangling bonds." A free cation and anion are shown in the top right and bottom left corner, respectively. Dotted lines encircling the different clusters have been used to clearly demark each cluster.

II. CHEMICAL EQUILIBRIUM CONSIDERATIONS

One of the first questions that arises when considering clustering in the EDL is what chemical equilibrium should hold? In the bulk, McEldrew *et al.*[64] established the equilibrium between l free cations and m anions with clusters of rank lm (in which there are l cations and m anions associated). This bulk cluster equilibrium, as seen in Fig. 2, was shown to agree with the cluster distribution independently computed from molecular simulations for ILs.[49] To study the EDL, there must be an equilibrium between ions near the interface and the bulk.

If a "standard approach" is taken for the EDL–bulk equilibrium, i.e., where the ions in the bulk are assumed to accumulate in the EDL based on a Poisson–Boltzmann or Poisson–Fermi distribution from the bulk concentrations,[80–83] the ions are not permitted to reversibly associate in the EDL.[56,59–61] Such approaches bring ions to the EDL based on the charge and volume of the ion, but once the species are in the EDL, no further change of the ionic associations can occur. Moreover, with such an approach, it is not clear how the gel phase, if it forms, should be treated, and assumptions about how it will respond to an electrostatic potential will be required. For example, the gel could be assumed to not respond to the potential/field, and it remains as a constant background (charge), similar to solid electrolytes.[84] However, the gel is not a rigid solid;[64] so, this approach would have shortcomings. Alternatively, an approach similar to how solvent is treated in the dilute electrolyte limit could be taken, i.e., the gel can be taken as some constant background dielectric, which would be trivially pushed out of the EDL based on how ions come to the EDL.[80,83]

In the bulk, the gel phase is in equilibrium with free ions, and changes to the physical variables (such as temperature) can cause the balance of the equilibrium to shift.[64] Therefore, to model the cluster equilibrium in the EDL, *we demand that the cluster distribution in the EDL has the same form as in the bulk* but is altered by the differing volume fractions of cations and anions in the EDL. An equilibrium between the bulk and EDL then needs to be established,
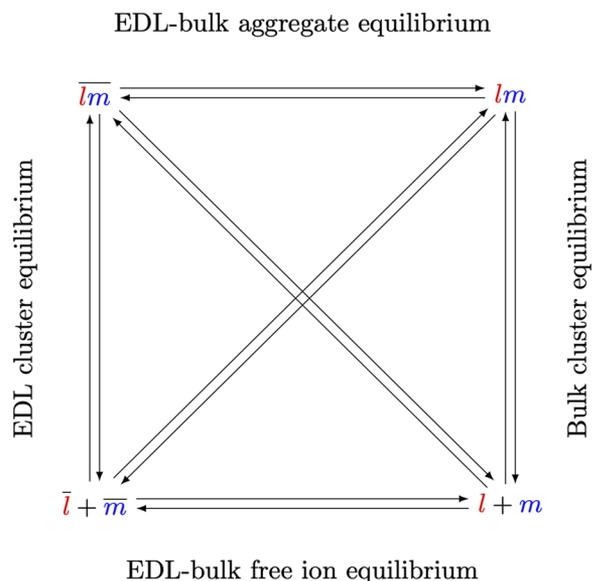
FIG. 2. Schematic depicting all possible chemical equilibria for thermoreversible associations between ions of an IL, in the bulk and EDL. Free cations in the bulk are denoted by l, and free anions m, which can form clusters of rank lm. This equilibrium is referred to as the bulk cluster equilibrium. An equivalent equilibrium should hold in the EDL, where barred quantities are used. There is also an equilibrium between the bulk and EDL.

FIG. 3. Schematic of changes to the clustering in the EDL. On the left, depicted is a negatively charged electrode, which polarized the EDL with a potential distribution decaying to the right. The same notation for the clusters as Fig. 1 is used, but where each ion can form a maximum of three associations.

which keeps both the bulk and EDL cluster equilibria consistent. Note only one of the four EDL–bulk equilibria (bulk free ions–EDL free ions; bulk free ions–EDL clusters; bulk clusters–EDL free ions; bulk clusters–EDL clusters) shown in Fig. 2 needs to be established for the remaining three to also hold. This approach should naturally show how the gel and all clusters respond to electrostatic fields, as a consequence of all chemical equilibria shown in Fig. 2 being held consistently.

III. PREVIEW

The results of this theory shall be briefly summarized, as there are conceptual advances here that are beneficial to bear in mind before the technical parts are introduced. Firstly, the main advancement this paper makes is the account of the *chemical equilibrium between clusters within the EDL*. Consideration of this equilibrium permits a natural way to investigate strongly aggregating and gelating electrolytes in the EDL.

This theory predicts the following. For electrolytes that do not contain a gel, the large clusters are broken down and expelled from the EDL in favor of free ions, as schematically shown in Fig. 3. The consideration of clusters beyond free ions results in a differential capacitance response that is larger than that of just a free ion approach. Overall, this is the expected result for the pre-gel regime, and it mainly differs from that of previous free ion theories (FIT) through quantitative measures.

For electrolytes that contain gel, the physical picture is more complex. It is found that *the gel can screen electrode charge*. This is because the g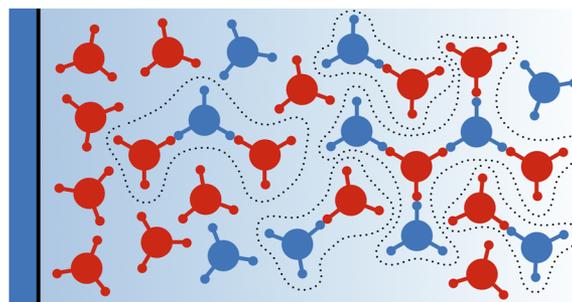el becomes charged in an electrostatic potential, with the gel being counterion dominated. This arises because the equilibrium between cation–anion associations changes in the EDL, where there are unequal numbers of cations/anions. For an accumulation of anions (cations) in the EDL, one finds that the gel is also negative (positive), because the equilibrium tries to shift back (Le Chatelier's principle) and remove some of the free anions (cations). Moreover, the cations (anions) are removed for positive (negative) potentials, which causes cations (anions) to dissociate from the gel to replenish the free cation (anion) concentration. At sufficiently large potentials, the ratio of cations/anions (anions/cations) in the EDL becomes small enough for the gel to be destroyed. This causes the gel to dissociate and release large aggregates.

For even greater values of the potential, these large aggregates are also broken down, and more and more free ions accumulate in the EDL, until the crowding regime is reached. Here, crowding refers to an electrolyte composition where practically only free counterions exist, which can be achieved locally in the EDL. Gradually, the excluded volume effect causes the thickness of the EDL to increase. Thus, the differential capacitance of the EDL, which is inversely proportional to the EDL thickness, starts decreasing at large potential drops across the EDL. At small voltages, however, the differential capacitance increases,[81,82] and, therefore, the capacitance curve will be a typical "double hump camel" shape overall.[81] Again, we find that accounting for the gel/cluster response increases and smooths out the response in comparison to a free ion theory.

Note that one must not expect the theory to provide the picture with "molecular resolution," explicitly showing overscreening oscillations of charge density and the spatial structure within clusters. Within the large clusters or the gel, alternation of counterions and coions should give rise to such oscillations. The presented theory is able to provide a "coarse-grained" structure of charge distribution in the EDL, spread over different clusters, the balance between which shifts with the polarization of the electrode. Needless to say, such theory will be thermodynamic, not covering any dynamic aspects of the EDL charging.

IV. THEORY
A. Ionic liquid associations

The limit of a symmetric, incompressible IL is employed here, i.e., one where the volumes of cations and anions are the same

$(v_+ = v_- = v)$, no voids are considered (every lattice site is either occupied by a cation or anion), and the number of associations a cation and anion can form is the same (referred to as functionality, given by $f_+ = f_- = f$). It is assumed that cations can only bind to anions, and anions to cations, i.e., no cation–cation and anion–anion associations are accounted for which has been shown to be a good approximation for ILs in Ref. 49. No interactions beyond ions that are directly associated are taken into account when determining the extent of associations (in the bulk). The ions are assumed to form Cayley tree clusters, i.e., ones in which there are no intra-cluster loops. Therefore, cations and anions can reversibly form "branched alternating co-polymers" of various sizes, from ion pairs to a percolating ionic network. These clusters/gel are schematically shown in Figs. 1 and 4.

Physically, these short-range associations between cations and anions in ILs represent the strong electrostatic correlations (beyond mean-field) between ions of opposite sign. Levy et al.[34] showed that the discrete charges of ions with a given packing (e.g., from molecular dynamics simulations) could be well reproduced by a nearest-neighbor spin-glass theory that maximizes their alternating-charge ordering, which implies that our short-ranged model of Coulomb correlations should be accurate for these concentrated electrolytes. Moreover, in Ref. 49, it was found that IL ions have well-defined "hot spots," where cations (anions) prefer to reside around anions (cations), which also supported these assumptions and permitted the functionality to be determined (from the number of hot spots).

ILs are the simplest possible super-concentrated electrolyte, and they should serve as a testing ground to investigate the EDL of

FIG. 4. Schematic of coexisting sol and gel. Cations and anions are shown in red and blue, respectively, and both have a functionality of 3. The percolating ionic network, i.e., the gel, is indicated by the enclosed dashed line. The remaining cations and anions are part of the sol. In the absence of the gel, all cations and anions are part of the sol.

electrolytes capable of forming associations beyond ion pairs. For further details about the IL limit, see Ref. 49.

The electrolyte is treated on the level of a lattice-gas.[49,64] The number of lattice sites, Ω, is given by

$$\Omega = \sum_{lm} (l + m) N_{lm} + N_+^{gel} + N_-^{gel}, \tag{1}$$

where N_{lm} is the number of clusters of rank lm and $N_{+/-}^{gel}$ is the number of cations/anions in the gel phase. The cations and anions that are not part of the gel, i.e., all of the free cations, free anions, and clusters of rank lm, are part of the *sol*. This is schematically shown in Fig. 4. In the absence of gel, all cations and anions are in the sol. Throughout, free ions and clusters shall not be explicitly referred to as being in the sol, as they are such by definition. Therefore, we do not explicitly include *sol* superscripts for free ions and clusters for clarity of notation.

Dividing Eq. (1) by the total number of lattice sites yields

$$1 = \sum_{lm} (l + m) c_{lm} + c_+^{gel} + c_-^{gel}, \tag{2}$$

where $c_{lm} = N_{lm}/\Omega$ is the dimensionless concentration (# per lattice site) of rank lm clusters, and the dimensionless concentration of cations/anions in the gel is $c_{+/-}^{gel} = N_{+/-}^{gel}/\Omega$, i.e., the volume fraction $c_{+/-}^{gel} = \phi_{+/-}^{gel}$. The volume fraction of a cluster of rank lm is given by $\phi_{lm} = (l + m) c_{lm}$. The volume fraction of cations and anions in the sol phase is

$$\phi_+^{sol} = \sum_{lm} l c_{lm}, \tag{3}$$

$$\phi_-^{sol} = \sum_{lm} m c_{lm}. \tag{4}$$

The total volume fraction of cations/anions is $\phi_{+/-} = \phi_{+/-}^{sol} + \phi_{+/-}^{gel}$. When there is no gel, the superscript *sol* shall be dropped for clarity of notation. In Fig. 4, the partitioning of the sol and gel is schematically shown.

The free energy of the cluster equilibrium[49,64] is taken to be

$$\beta \mathcal{F} = \sum_{lm} [N_{lm} \ln(\phi_{lm}) + N_{lm} \Delta_{lm}]$$
$$+ \Delta_+^{gel} N_+^{gel} + \Delta_-^{gel} N_-^{gel}, \tag{5}$$

where $\beta = 1/k_B T$ is the inverse thermal energy, Δ_{lm} is the free energy of formation of a cluster of rank lm from free cations and anions, and $\Delta_{+/-}^{gel}$ is the free energy change of cations/anions associating with the gel.

Establishing chemical equilibrium,[49,64,66] as shown in the supplementary material, the cluster distribution is expressed as

$$c_{lm} = \frac{W_{lm}}{\lambda} (\lambda f \phi_{10})^l (\lambda f \phi_{01})^m, \tag{6}$$

where $\lambda = \exp(-\beta \Delta f_{+-})$ is the ionic association constant, with $\Delta f_{+-} = \Delta u_{+-} - T \Delta s_{+-}$ denoting the free energy of an association, determined by the binding energy (Δu_{+-}) and (configurational)
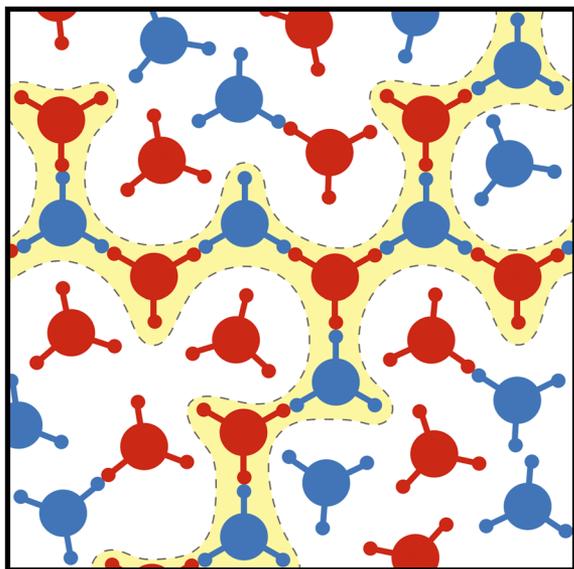
entropy of an association (Δs_{+-}). Here, W_{lm} is the number of ways to arrange l cations and m anions in a Cayley tree,[49,64] i.e., the combinatorial contribution to the free energy of formation of a cluster, which is given by

$$W_{lm} = \frac{(fl-l)!(fm-m)!}{l!m!(fl-l-m+1)!(fm-m-l+1)!}. \tag{7}$$

The cluster distribution, c_{lm}, is expressed in terms of ϕ_{10} and ϕ_{01}; but, in principle, these are unknown quantities. In the bulk, the volume fraction of cations and anions is, however, known. Introducing association probabilities, p_{ij}, the probability that an association site of species i is bound to species j, permits the volume fraction of free cations to be written as $\phi_{10} = \phi_+(1-p_{+-})^f$ and that of free anions as $\phi_{01} = \phi_-(1-p_{-+})^f$.

The association probabilities can be determined through conservation of associations, i.e.,

$$f\phi_+ p_{+-} = f\phi_- p_{-+} = \zeta, \tag{8}$$

and mass action law given by

$$\lambda\zeta = \frac{p_{+-}p_{-+}}{(1-p_{+-})(1-p_{-+})}, \tag{9}$$

to give the probability of cations binding to anions,

$$p_{+-} = \frac{1+f\lambda - \sqrt{1+2f\lambda+f^2\lambda^2(1-2\phi_+)^2}}{2f\lambda\phi_+}, \tag{10}$$

and that of anions binding to cations,

$$p_{-+} = \frac{1+f\lambda - \sqrt{1+2f\lambda+f^2\lambda^2(1-2\phi_-)^2}}{2f\lambda\phi_-}. \tag{11}$$

Note that the volume fractions have been explicitly retained in these equations, as these probabilities can be investigated as a function of the volume fraction of cations and anions.

When the probability of a cation (anion) having another cation (anion) connected through an anion (cation), reaches 1 a percolating ionic network can form. This condition is given by $1 = (f-1)^2 p_{+-}^* p_{-+}^*$, where the stars are used to denote the critical probabilities for the formation of the percolating ionic network. When the probabilities reach this condition, the volume fractions of cations and anions in the gel and sol must be determined. Flory's treatment of the post-gel regime is employed, in which the volume fraction of free ions can be written equivalently in terms of overall association probabilities, p_{ij}, and association probabilities taking into account only the species residing in the sol, p_{ij}^{sol},

$$\phi_+(1-p_{+-})^f = \phi_+^{sol}(1-p_{+-}^{sol})^f, \tag{12}$$

$$\phi_-(1-p_{-+})^f = \phi_-^{sol}(1-p_{-+}^{sol})^f. \tag{13}$$

Using Eqs. (12) and (13) in addition to Eqs. (8) and (9), with sol-specific quantities, permits the determination of the sol probabilities and volume fractions. The fraction of species, i, in the sol is given by $w_i^{sol} = \phi_i^{sol}/\phi_i$. See the supplementary material for more details.

B. Cluster/gel composition of ILs

Having summarized the equations for the cluster equilibrium, we turn to understanding the behavior of the system with unequal volume fractions of cations and anions. In principle, one cannot arbitrarily control the volume fractions of cations or anions. The charge of an electrode sets the number of excess counter charges that must be in the EDL, to have overall charge neutrality. These charges shall be distributed in space according to the Poisson equation. However, it is quite useful for conceptual understanding to perform a thought experiment where one can change the volume fraction of cations/anions arbitrarily. Therefore, we shall investigate the composition of the electrolyte as a function of the volume fraction of cations. To start, we shall briefly summarize the composition of the electrolyte in the bulk, i.e., where $\phi_+ = \phi_- = 1/2$, for $\lambda = 1$ and $\lambda = 10$, with $f = 3$. Then, we shall progress onto investigating $\phi_+ \neq \phi_-$.

1. Bulk composition

In the bulk, the critical value of the association constant for the formation of the gel is given by $\lambda^* = 2(f-1)/[f(f-2)^2]$. For $f = 3$, this puts $\lambda^* = 4/3$, which means the chosen association constants are on either side of the gel point. These two different values of λ, 1 and 10, can be considered as an example of those at a high and low temperature, respectively.

For larger functionalities, $\lambda^* < 1$, which might be surprising, as this corresponds to a positive free energy of an association, Δf_{+-}. It was found in Ref. 49, from the temperature dependence of the association constant, that the binding energy is negative, but the entropy of an association is also negative, which may result in $\Delta f_{+-} > 0$. The reason why a gel can form with $\lambda < 1$, and why there are still significant associations despite $\Delta f_{+-} \geq 0$, can be understood in several ways. The free energy of an association, Δf_{+-}, is not the only contribution to the free energy of formation of clusters of rank lm, there are additional entropic contributions (combinatorial entropy and part of the configurational entropy—see Refs. 49 and 64 for more details) that drive the system toward a mixture rather than a pure state (of free ions). This has also been found by Lee et al.[52] when considering ion pair formation in ILs, where 2/3 of ions were found to be free. This was because the Debye screening length was much shorter than the radius of an ion, and, therefore, there was no enthalpic benefit for the formation of ion pairs, which meant the entropy of mixing decided the fraction of free ions, i.e., the IL was effectively treated as an ideal solution. Alternatively, this can be understood from the mass action law, Eq. (9), which shows that the association probabilities only vanish when $\lambda = 0$. The association constant is effectively the equilibrium constant of the formation of an association, which means that when $\lambda = 1$, it is equally favorable to form an association as not to, and, therefore, entropy maximization dictates that a mixture shall form. As the entropy of an association was found to be positive in Ref. 49, the association constant tends to 0 at large temperatures, which is the expected limit of no associations. Note that associations between cations–anions still occur, although $\Delta f_{+-} > 0$, due to the negative binding energy.

Having described the extent of associations for different λ, we turn to understanding the cluster distribution in more detail. In Fig. 5, the volume fraction of each cluster of rank lm is shown as a function of the size of each cluster ($l + m$) for the bulk $\phi_+ = \phi_- = 1/2$
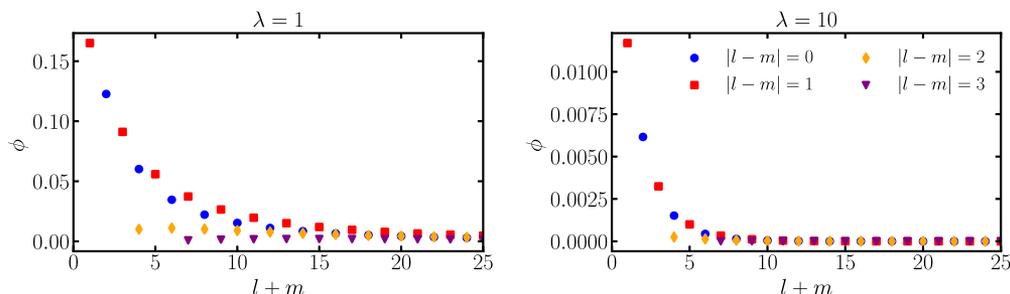
FIG. 5. The composition of the bulk IL is dominated by neutral and singly charged clusters. Volume fraction of each rank of cluster, for a given charge $|l - m| = q$, with $q = 0, 1, 2, 3$ and $f = 3$, as a function of the size of a cluster $l + m$.

with $f = 3$. This is plotted for various overall charges of clusters, with charges up to ± 3 being considered. As it is the symmetric case, the volume fraction of a $+q$ charged cluster is equal to the $-q$ charged clusters. Therefore, these are summed together, and each different symbol represents a $|l - m| = q$, for $q = 0, 1, 2, 3$.

For $\lambda = 1$, see Fig. 5 (left), the IL is in the pre-gel regime. There is ~16% of free ions, with the remaining fraction of ions being bound up into clusters. The neutral ion pairs are the next most populous species, followed by singly charged triples, etc. These singly charged and neutral clusters dominate the electrolyte composition (for a symmetric IL in the bulk[64]). A cluster with $|l - m| = 2$ can first occur when there are four ions in the cluster. The volume fractions of these clusters initially increases slightly with $l + m$, since for larger $l + m$, not all association sites must be occupied (unlike $l + m = 4$ for $f = 3$), before decreasing again for large cluster ranks. A similar story occurs for $|l - m| = 3$, where it is found to have even smaller volume fractions.

For $\lambda = 10$, see Fig. 5 (right), the IL is in the post-gel regime, with most of the ions being bound in the gel. For the remaining clusters, a similar situation can be seen for the populations of clusters. For more information about the bulk cluster composition of an IL, see Ref. 49.

2. "EDL" composition

In Fig. 6 (left), the association probabilities as a function of volume fraction of cations is shown, for $\lambda = 1$ with functionality of $f = 3$. As the volume fraction of cations increases, the association probability of cations binding to anions (p_{+-}) decreases and the

association probability of anions binding to cations (p_{-+}) increases. The opposite is true for a decreasing volume fraction of cations. This is a consequence of the conservation of associations, which states $p_{+-}/p_{-+} = \phi_-/\phi_+$. At $\phi_+ = 1$, the association probability of cations binding to anions necessarily goes to zero, $p_{+-} = 0$, and p_{-+} reaches a constant value equal to or less than 1, and vice versa for $\phi_+ = 0$.

For $\lambda = 10$, the association probabilities are sufficiently large to create a percolating ionic network in the bulk, as seen by $p_{+-}p_{+-}$ being larger than the dashed horizontal line in Fig. 6 (right). Again, p_{+-} decreases with increasing ϕ_+ and p_{-+} increases with increasing ϕ_+. There comes a point, for both small and large ϕ_+, that the volume fraction of cations (or anions) cannot sustain a percolating ionic network, and $p_{+-}p_{+-}$ drops underneath the threshold.

Next, how these association probabilities influence the cluster distribution of the electrolyte is shown in Fig. 7 as a function of the volume fraction of cations. For $\lambda = 1$, the volume fraction of free cations (ϕ_{10}) increases with the volume fraction of cations (ϕ_+) and the volume fraction of free anions (ϕ_{01}) decreases with increasing ϕ_+. At $\phi_+ = 1$, $\phi_{10} = 1$ and $\phi_{01} = 0$, and vice versa for $\phi_+ = 0$. This is a reflection of the changing association probabilities and volume fractions, as just discussed. The volume fraction of ion pairs (ϕ_{11}) and aggregates beyond ion pairs ($\phi_{lm>11}$) decreases for increasing and decreasing volume fractions of cations (relative to its bulk value). This is because the average association probability, $(p_{+-} + p_{-+})/2$, decreases as the volume fractions of cations is changed from the bulk value.

For $\lambda = 10$, the volume fraction of free cations and free anions behaves in an analogous manner to that for the case of $\lambda = 1$, and the volume fraction of ion pairs is always extremely small.
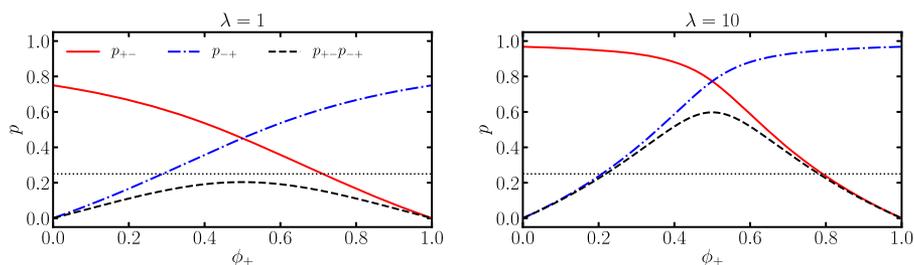
FIG. 6. The IL becomes less associating as the volume fractions of cations increases/decreases from the bulk value. Association probabilities, as indicated in the legend, as a function of volume fraction of cations. Two association constants are shown, as indicated in the titles. Both plots are for a functionality of 3, and the horizontal dotted line denotes the critical probability for the onset of a gel, $p_{+-}^* p_{-+}^* = (f - 1)^{-2}$.
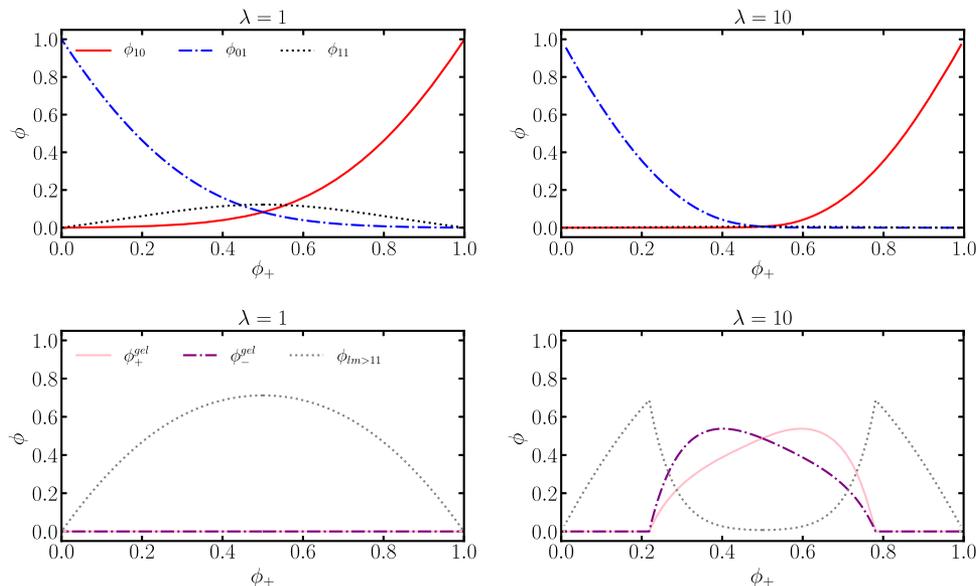
FIG. 7. Free ions become increasingly dominant and the gel is destroyed for sufficiently charged systems. Volume fractions of free cations (ϕ_{10}), free anions (ϕ_{01}), and ion pairs (ϕ_{11}) as a function of the volume fraction of cations (top panels). Volume fractions of aggregates beyond ion pairs ($\phi_{lm>11}$), volume fraction of cations in the gel (ϕ_+^{gel}), and volume fraction of anions in the gel (ϕ_-^{gel}) as a function of volume fraction of cations (bottom panels). Again, all plots are for $f = 3$ and the two association constants are shown in the titles.

The aggregates beyond ion pairs behave qualitatively differently, however, with a highly non-monotonic dependence on ϕ_+. To understand this, the behavior of the gel must first be described. In the bulk, the system is significantly gelled. As the volume fraction of cations increases (ϕ_+), the volume fraction of cations in the gel (ϕ_+^{gel}) also increases and the volume fraction of anions in the gel (ϕ_-^{gel}) decreases. This is because the prevalence of cations shifts the free ion–gel equilibrium to accommodate more cations. Therefore, *the gel becomes charged and decreases in total volume fraction*, until it reaches the critical volume fraction where it can no longer be sustained. This decreasing volume fraction of gel causes a dramatic increase in the volume fraction of aggregates beyond ion pairs, as closer to the gel point, larger and larger clusters dissociate from the gel. When the critical volume fraction to sustain a gel is reached, there is no longer gel to create large clusters, and the decreasing average association probability causes a dramatic decrease in the volume fraction of these larger clusters.

Overall, the phenomenology described in this thought experiment is exactly what is expected for the behavior of the clusters in the EDL: a transition from gelation/aggregation to crowding. Therefore, what is required is a connection between the volume fractions of cations/anions and the electrostatic potential, which can be linked to the spatial distribution of charges through the Poisson equation.

Inspecting the equations for $p_{\pm\mp}$ and $\phi_{10/01}$ demonstrates that, for a given volume fraction of cations, the volume fractions of free anions and free cations are not independent, but they are constrained by the associations. Therefore, if EDL–bulk equilibrium was established with "standard approaches," such as Boltzmann or Fermi functions for free cations and free anions, the system of equations (the above equations for the concentrations of each species and the Poisson equation) becomes overdetermined and the cluster distribution is no longer consistent. Therefore, an alternative approach to investigate the EDL properties in a consistent way is sought.

In the supplementary material, this is shown explicitly from the free energy. Moreover, alternative approaches to make the cluster distribution consistent everywhere is outlined.

It is interesting to note that this observation also applies to approaches, such as Refs. 60 and 61, where the associations were only treated through the explicit treatment of the remaining free ions. In the bulk, the number of free ions was determined by the binding free energy of cations and anions. The bulk concentration of free cations and free anions was then utilized in a Poisson–Fermi theory for the EDL.[56,58,59,61] This essentially treated the associations as irreversible in the EDL, but reversible in the bulk, which is also how Ref. 51 investigated strongly associating ILs within a sophisticated classical density functional theory. For thermoreversible associations in the EDL, the number of associations based on the concentration of cations and anions must also be determined in the EDL. This deficiency in such approaches[56,58,59,61] does not, however, qualitatively change the predictions of those theories in terms of the free ions.

C. Boltzmann closure of free ions

To close the system of equations without overdetermining, a single relationship is required to connect the electrostatic potential with the volume fractions. To achieve this, the following closure relationship is taken based on the ratio of free cations and free anions in the EDL

$$\frac{\phi_{10}}{\phi_{01}} e^{-2\alpha u} = \frac{\bar{\phi}_{10}}{\bar{\phi}_{01}} = \frac{\bar{\phi}_+ (1 - \bar{p}_{+-})^f}{\bar{\phi}_- (1 - \bar{p}_{-+})^f}, \tag{14}$$

where the bar has been used to indicate quantities in the EDL and u is the electrostatic potential in units of thermal voltage (which is given by $1/\beta e$, with e denoting the elementary charge, i.e., the magnitude of the charge of an ion studied here). The factor α is a parameter that describes additional correlations beyond mean-field

electrostatics (defined such that $0 \leq \alpha \leq 1$), as introduced in Ref. 59, and shown to work well in Ref. 85. Since λ accounts for short-ranged attractive interactions between cations–anions, only the short-ranged repulsion between cations–cations/anions–anions are considered in α. This prevents double counting the short-ranged attraction between cations–anions. Moreover, α is not assumed to be based on the free ion fractions, but the total ion fractions, since the gel can also become charged. This parameter acts to smooth out the response of ions to the electrostatic potential, as the Poisson–Boltzmann (or Fermi) distribution is well known to overestimate the response.[80,83] This is analogous to the dressed ion theory, where the charge of an ion is rescaled to smaller values because of correlations between ions.[38]

Equation (14) assumes that free ions behave in a Boltzmann way while being consistent with the cluster distribution and incompressibility constraint. This expression can be used to solve for the local volume fraction of cations or anions within the EDL, which then determines the local free cation and free anion volume fractions. These can be used in the cluster distribution given by

$$\bar{c}_{lm} = \frac{W_{lm}}{\lambda} \left(\lambda f \bar{\phi}_{10} \right)^l \left(\lambda f \bar{\phi}_{01} \right)^m,$$ (15)

to find the concentrations of all clusters. Moreover, when the free cation/anion volume fractions are known, so are the association probabilities. This means that the gel can also be treated in a consistent way.

For $\lambda \ll 1$, the association probabilities tend to zero $p_{+-} = p_{-+} \approx 0$, which means $\bar{\phi}_+/\bar{\phi}_- \approx e^{-2\alpha u}$. Using the incompressibility condition, this can be solved to give $\bar{\phi}_+ - \bar{\phi}_- = -\tanh \alpha u$ for the charge density, which is the expected result when there are no associations.[81,82]

1. Linear response

When there are associations, the approach cannot generally be solved analytically, but at linear response, some insight can be gained. Taking a linear expansion of Eq. (14) and introducing a symmetric perturbation of free ions, $\bar{\phi}_{10} = \phi_{10} + \delta\bar{\phi}_f$ and $\bar{\phi}_{01} = \phi_{01} - \delta\bar{\phi}_f$, yield $\bar{c}_{10} = c_{10}(1 - \alpha u)$ for the free cation concentration and $\bar{c}_{01} = c_{01}(1 + \alpha u)$ for the free anion concentration. Using this in the cluster distribution yields

$$\bar{c}_{lm} = c_{lm}[1 - (l - m)\alpha u].$$ (16)

Introducing the EDL volume fraction and probabilities as the bulk perturbed by a small value, $\bar{\phi}_\pm = 1/2 \pm \delta\bar{\phi}$ and $\bar{p}_{\pm\mp} = p \pm \delta\bar{p}$, respectively, the volume fraction of cations changes by

$$\delta\bar{\phi} = \frac{-(1-p)\alpha u}{2[1 + (f-1)p]},$$ (17)

where $p = (1 + f\lambda - \sqrt{1 + 2f\lambda})/f\lambda$ is the association probability in the bulk.

Therefore, the Poisson equation takes the form

$$\nabla^2 u = \frac{e^2 \beta \alpha u}{v\epsilon_0 \epsilon} \sum_{lm} (l-m)^2 c_{lm} = \frac{e^2 \beta \alpha u}{v\epsilon_0 \epsilon} \frac{(1-p)}{[1 + (f-1)p]},$$ (18)

where ϵ_0 and ϵ are the permittivity of free space and relative permittivity, respectively, and v is the volume of an ion (i.e., a lattice site). The screening length given by

$$\ell = \frac{1}{\sqrt{\alpha}\kappa} \sqrt{\frac{1 + (f-1)p}{(1-p)}}$$ (19)

is based on the ionic strength of the cluster distribution, with $\kappa = \sqrt{v\epsilon_0\epsilon/e^2\beta}$. When there are no associations, i.e., $p = 0$, the Debye length is recovered. In the opposite limit, the association probability tends to 1, and extremely large screening lengths can emerge. This expression for the ionic strength in terms of p was previously derived in Ref. 49 from modifying the expression for the weight average degree of aggregation. Therefore, the Boltzmann closure of free ions appears to be well justified at linear response in the pre-gel regime.

Gebbie *et al.*[36,37] have suggested that ILs screen the field in a Boltzmann way with few free ions. Thus, this closure relation could also be assumed to hold in the post-gel regime. This would mean the screening length in Eq. (19) also holds in the post-gel regime, because it can be derived from the total volume fractions and probabilities. The contribution to this screening length from the clusters and gel can be derived. Again, a symmetric perturbation for the change in volume fractions of sol ($\delta\bar{\phi}_+^{sol} = -\delta\bar{\phi}_-^{sol} = \delta\bar{\phi}^{sol}$) and sol probabilities ($\delta\bar{p}_{+-}^{sol} = -\delta\bar{p}_{-+}^{sol} = \delta\bar{p}^{sol}$) is introduced. In the system of equations, there are two unknowns, $\delta\bar{\phi}^{sol}$ and $\delta\bar{p}^{sol}$; therefore, two equations are required. One of these equations is Flory's treatment of the post-gel regime; the second equation is the conservation of associations in the sol. Solving these equations, while using the previous results for $\delta\bar{\phi}$ and $\delta\bar{p}$, gives

$$\delta\bar{\phi}^{sol} = -\frac{w^{sol}(1 - p^{sol})\alpha u}{2[1 + (f-1)p^{sol}]},$$ (20)

which is an analogous expression for the sol quantities. Therefore, the change in the volume fraction of the gel is given by

$$\delta\bar{\phi}^{gel} = -\frac{\alpha u}{2} \left\{ \frac{(1-p)}{1 + (f-1)p} - \frac{w^{sol}(1 - p^{sol})}{1 + (f-1)p^{sol}} \right\}.$$ (21)

These results can be used to decompose the total screening length into the contributions from the sol and the gel.

In Fig. 8, the dimensionless ionic strength, $(\kappa\ell)^{-2} = \sum_{lm} (l-m)^2 c_{lm}$ (taking $\alpha = 1$), is shown as a function of the association constant. For $\lambda < \lambda^*$, where the star is used to denote the critical association constant for the formation of the gel, the ionic strength is determined by the clusters. For an association constant just above the critical value, both clusters in the sol and the gel contribute to the screening at linear response. For $\lambda \gg \lambda^*$, practically only the gel contributes to the screening at linear response. This indicates that approaches based on free ions,[60,61] which follow the sol contribution closely,[49] underestimate the ability of the electrolyte to screen.
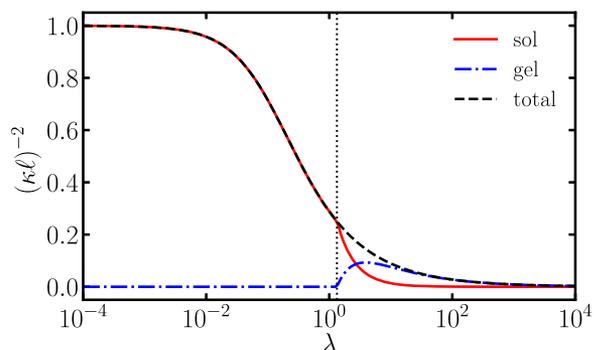
FIG. 8. The ionic strength decreases with association constant, but in the post-gel regime, the gel dominates the ionic strength. Dimensionless ionic strength, given by $1/(\kappa\ell)^2$, as a function of association constant, λ, for $f = 3$. Note the x axis is on a logarithmic scale. The α parameter is set to 1.

2. Nonlinear response

Generally, the differential equation that needs to be solved is given by

$$\nabla^2 u = -\kappa^2 \left[\sum_{lm}(l-m)\bar{c}_{lm} + \bar{c}_+^{gel} - \bar{c}_-^{gel} \right] = -\kappa^2 \left[\bar{\phi}_+ - \bar{\phi}_- \right]. \quad (22)$$

A constant charge boundary condition at the interface is taken and a zero electrostatic potential in the bulk is used. Numerical results for the solution to this nonlinear differential equation shall be shown in Sec. V. Note that a Stern layer is not considered here for clarity of discussing the new results. In the supplementary material, a step-by-step guide of how to implement the equations to obtain a numerical solution is given.

V. RESULTS

A. EDL structure

To start, the description of the nonlinear solution to Eq. (22) in terms of the electrostatic potential and charge density shall be outlined. The results for these are shown in Fig. 9 as a function of distance from an interface that has a charge of 0.02 Cm^{-2} for the studied

association constants. Both the electrostatic potential (in units of thermal voltage) and charge density (in units of the charge per unit lattice site) are found to monotonically decay from the interface, as expected from a local density approximation.

For $\lambda = 1$, the potential and charge density decay to the bulk values within $\sim 30/\kappa$. The crowding regime, defined by $c_{01/10} \approx 1$ and $c_{10/01} \approx 0$, which has to be taken here because an incompressible IL can only accumulate charge density, not number density in the EDL, can clearly be seen, since the dimensionless charge density reaches -1 at the interface. For $\lambda = 10$, the electrostatic potential and charge density decay further from the interface, owing to the larger screening lengths from more associations. The crowding regime is also reached near the interface, as can be seen from the charge density reaching -1. These results are expected, and we can now turn to decomposing the charge density into the different contributions to understand the response of the IL further.

In Fig. 10, the charge density of Fig. 9 is decomposed into the free ions, ion pairs, clusters beyond ion pairs, and cations and anions in the gel. For $\lambda = 1$, free anions substantially increase close to the interface, where the crowding regime is reached. The free cations are expelled from the EDL rapidly. Both ion pairs and finite aggregates beyond ion pairs are depleted at length scales between the crowding regime of free anions and the expulsion of free cations. This is because it is more favorable to have the free ions in the EDL than clusters.

For $\lambda = 10$, the structure of the EDL is more complicated. At short distances from the positively polarized electrode, the free anions again reach the crowding regime. The free cations and ion pairs are practically zero in the bulk and do not appear to change much in the EDL. For increasing distances from the interface, $\phi_{lm > 11}$ initially increases, as the number of cations/anions starts to equalize, which permits the large aggregates to be created. This occurs until the gel point is reached, where the large clusters combine. For further distances, there is a significant volume fraction of gel, but the number of cations and anions in the gel are not equal. There are more anions in the gel than cations, which means the gel screens the field. In fact, in this regime, the field is practically only screened by the gel, since the volume fraction of free anions is much smaller. Again, the gel can screen the electrostatic potential because of the shift in the equilibrium between how the free ions associate to the gel when there are unequal numbers of cations/anions.
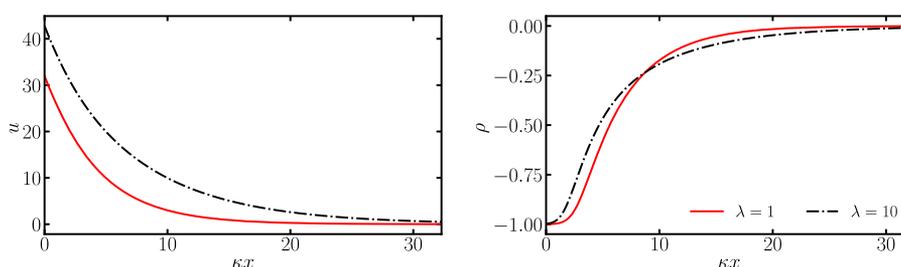
FIG. 9. Monotonic behavior and decay of electrostatic potential and charge density. Electrostatic potential in units of thermal voltage (left panel) and charge density in units of charge per lattice site (right panel) in the EDL as a function of the interface for a surface charge density of 0.02 Cm^{-2}. All calculations are for $f = 3$ and $\alpha = 0.2$ at the two association constants shown. For $T = 300$ K, $v = 1$ nm^3, $\epsilon = 5$, the inverse screening length is $\kappa \approx 0.85$ Å, which means the EDL structure is of a similar length scale to the size of an ion.

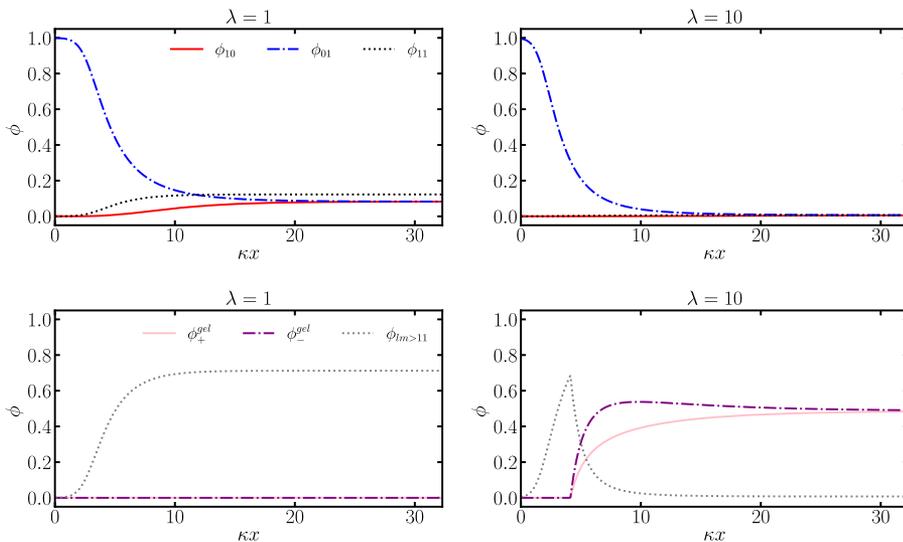**FIG. 10.** For strongly associating ILs, the gel can screen the electrode charge, but only far from the interface, as crowding of free ions near the interface dominates. Volume fractions in the EDL as a function from the interface for a surface charge density of 0.02 Cm^{-2}. Top panels show the volume fraction of free cations (ϕ_{10}), free anions (ϕ_{01}), and ion pairs (ϕ_{11}). The bottom panels show the volume fractions of finite aggregates beyond ion pairs and the volume fraction of cations in the gel and volume fraction of anions in the gel. These calculations were performed with the same parameters as Fig. 9.

B. Differential capacitance

The differential capacitance, C, can be calculated numerically within this theory through

$$\frac{C}{C_0} = \frac{d\tilde{\sigma}}{du_0}, \quad (23)$$

where $\tilde{\sigma}$ is the dimensionless surface charge density, $C_0 = \epsilon_0 \epsilon \kappa$ is the Debye capacitance without associations, and u_0 is the dimensionless potential drop across the entire EDL. When $\lambda \approx 0$, i.e., all free ions, and $\alpha = 1$, the differential capacitance numerically calculated within the presented theory exactly reproduces that of Refs. 81 and 82.

In Fig. 11, the numerical differential capacitance as a function of potential is plotted (solid line) alongside the analytical expression derived in Ref. 59,

$$\frac{C}{C_0} = \sqrt{\alpha\gamma} \frac{\cosh(\alpha u_0/2)}{1 + 2\gamma \sinh^2(\alpha u_0/2)} \sqrt{\frac{2\gamma \sinh^2(\alpha u_0/2)}{\ln\{1 + 2\gamma \sinh^2(\alpha u_0/2)\}}}, \quad (24)$$
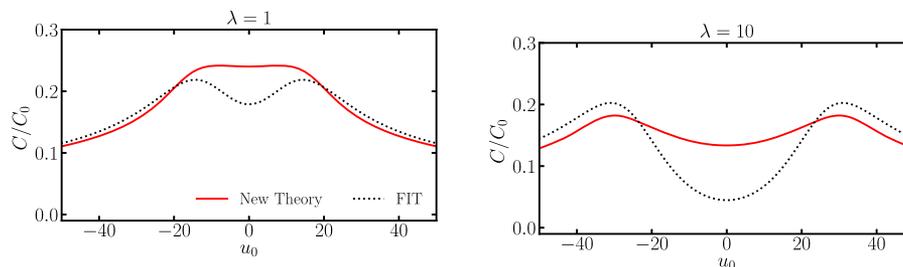
where γ is the free ion fraction based on a similar free ion fraction (dotted line) to the cluster distribution, where the additional factor of $\sqrt{\alpha\gamma}$ comes from the definition of κ taken here. Note that the treatment in Ref. 60 is based on just the free ions in an IL, referred to as a free ion theory (FIT), where there are only thermoreversible associations in the bulk.

For $\lambda = 1$, the free ion fraction is ~0.16, which is used in Eq. (24) of the FIT. Since the free ion fraction is smaller than 1/3, a clear "camel"[81] shaped differential capacitance curve is obtained from Eq. (24), i.e., initially the differential capacitance increases (in the overscreening regime) before a maximum is reached, after which the differential capacitance is governed by universal charge conservation laws.[81] In contrast, the numerical solution for the theory presented here only has a slight "camel" shape, with the differential capacitance at zero charge also being larger than the FIT.

For $\lambda = 10$, the free ion fraction is found to be ~0.01. Again, the FIT has a significant U-shape near the potential of zero charge, which goes through a maximum before the crowding regime is reached and the differential capacitance decreases (note that the

FIG. 11. Account of clusters beyond free ions in the EDL causes the capacitance at zero charge to increase, and the curves become more bell-like. Differential capacitance in units of Debye capacitance without associations, $C_0 = \epsilon_0 \epsilon \kappa \approx 75$–$100 \ \mu$Fcm^{-2}, as a function of voltage in units of thermal voltage (25.6 mV at room temperature). The solid (red) line corresponds to the differential capacitance computed numerically for the theory presented here. The dotted (black) line corresponds to the expression in the free ion theory (FIT) of Ref. 60 with free ion fractions, γ, of 0.16 and 0.01 for $\lambda = 1$ and $\lambda = 10$, respectively. All curves are plotted for $\alpha = 0.2$.

differential capacitance follows $C/C_0 \propto 1/\sqrt{u_0}$ for $u_0 > 40$, which is where $|\rho| = 1$ reaches in Fig. 9 and, therefore, the employed definition of the crowding regime is reasonable). The new theory presented here, in contrast, only has a slight "camel" shape, which is stretched out over the potential range, and again has a larger differential capacitance at zero charge.

Overall, there are two different features of the theory presented here against that of Ref. 60: (1) The screening length obtained here is always smaller than that given by Eq. (24) because larger clusters are explicitly accounted for. Therefore, the capacitance at zero charge is always larger. (2) The breakdown of clusters and gel causes the crowding regime to be reached at smaller potentials than that of Eq. (24), which makes the "camel" shape less pronounced.

The two association constants investigated here can be considered to be at two different temperatures for the same IL, since they are related to the free energy of an association through $\lambda = \exp\{-\beta \Delta f_{+-}\}$. Therefore, larger temperatures correspond to smaller λ. As found in Ref. 60, we also observe a transition from a camel to bell shape with increasing temperature, owing to the dissociation of ions. Moreover, the capacitance at zero charge increases with decreasing associations because there are more charge carriers to screen the potential.

1. Comparison to experiments

In Ref. 49, it was found that both the cation and anion in 1-ethyl-3-methylimidazolium bis(trifluoromethylsulfonyl) imide [Emim][TFSI] have a functionality of 4 and that the volumes of each ion are practically the same. This is perhaps as close as one can get to the symmetric IL, which the new theory is applicable to. ILs are typically composed of ions with very different volumes and unequal functionalities.[49] Further development of the presented formalism is required to make predictions of asymmetric ILs.

In Ref. 86, Jitvisate and Seddon reported the experimental differential capacitance curves of various ILs, including [Emim][TFSI]. The data from Ref. 86 for [Emim][TFSI] have been reproduced in Fig. 12. A slight camel shape is found for [Emim][TFSI], with the wings of the capacitance curve at large voltages being approximately symmetric. It was noted in Ref. 86 that the differential capacitance curve could be approximately fitted with Eq. (24) using $\alpha \approx 0.07$ and $\gamma \approx 0.27$. If γ is interpreted as the free ion fraction, there would have been slightly less than 1/3 of free ions. This was also the conclusion of Ref. 60, based on fitting the differential capacitance curve obtained from molecular dynamics simulations. However, in Ref. 62, the fraction of free ions of [Emim][TFSI] was found to be only ~0.15 at room temperature, which is approximately half of that based on Ref. 60.

In Fig. 12, the differential capacitance curve from the new theory and the free ion theory (FIT), i.e., Eq. (24), is shown. The new theory can reproduce the differential capacitance curve reasonably well with $\lambda = 0.6$, as seen in Fig. 12. For $\lambda = 0.6$, the free ion fraction is 0.12, which is close to that of Ref. 62. For the FIT with a free ion fraction of $\gamma = 0.12$, the differential capacitance curve cannot reproduce experimental data well, being too "camel" shaped. The FIT with the fitted value of $\gamma = 0.27$ from Jitvisate and Seddon[86] is also shown for comparison. Therefore, the new theory appears to be able to rationalize the results[62,86] that were not in quantitative agreement before.
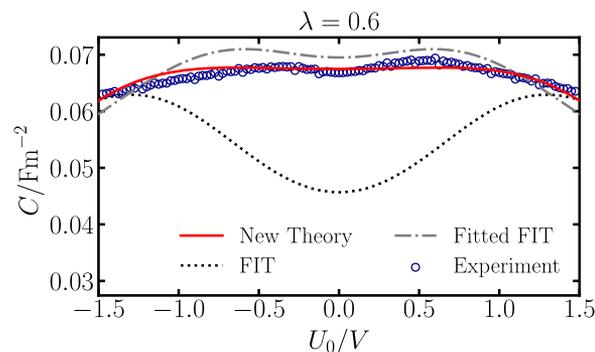

FIG. 12. Better agreement between experimental differential capacitance and the new theory compared to the free ion theory (FIT), using an independently determined free ion fraction. Differential capacitance as a function of potential drop across the EDL. The presented theory is shown by the solid red line and the theory of Eq. (24) is shown by the dotted black line, using the independently determined free ion fraction. A fitted $\gamma = 0.27$ for the FIT is also shown. The IL is taken to have $f = 4$ and an association constant of $\lambda = 0.6$ ($\gamma = 0.12$), with T = 298 K, maximal concentration of 7.76M, $\alpha = 0.07$[86] and dielectric constant of $\epsilon = 1$ (used as a parameter to reduce the capacitance at zero charge). The experimental values for [Emim][TFSI] are shown by open circles and have been reproduced from Ref. 86.

There are still a couple of free parameters, other than the free ion fraction that was independently taken to be close to Ref. 62, evaluated to obtain the differential capacitance curve in Fig. 12. One of these parameters is $\alpha = 0.07$, which was the value fitted by Jitvisate and Seddon.[86] Using this parameter and setting the dielectric constant to the bulk value (for [Emim][TFSI] this is $\epsilon = 12$[86]), one obtains a capacitance at zero charge that is too large. Therefore, to obtain a similar capacitance at zero charge, the dielectric constant is set to $\epsilon = 1$. As such value is unphysical (at least the polarizability of electronic degrees of freedom ions would contribute the value of 2), such fitting of ϵ demonstrates a shortcoming of the simple, local theory presented here and motivates further improvement. Note, to permit a transparent comparison with Jitvisate and Seddon,[86] a Stern layer has not been included, which would have reduced the capacitance at zero charge.

VI. DISCUSSION

A. Underscreening

The presented theory has implications for the interpretation of the experiments in Refs. 35–42. Inverting the expression for the screening length in terms of the association probability, we obtain

$$p = \frac{(\ell \kappa)^2 - 1}{f - 1 + (\ell \kappa)^2}. \quad (25)$$

In experiments,[35] the screening length multiplied by the inverse Debye length is $\ell \kappa \approx 100$ for ILs. Using this value yields an association probability of 0.9997 for a functionality of 3. This association probability produces ~3×10^{-11} free ions, *with the rest being gel*, which corresponds to a λ in excess of 1×10^6 and $\Delta f_{+-} \approx -14/\beta$. At large distances from the charged interface, we have found that

it is *actually the gel which screens the long-tail in electrode charge, not the free ions*. This could suggest that ILs are not dilute electrolytes, but a gel that can screen electrode charge. In fact, Jurado *et al.*[41,42] found 1-hexyl-3-methyl-imidazolium ethylsulfate forms lamellar-like structures on charged mica surfaces, (actually, speculated about already in Ref. 81) which are conceptually similar to the gel, albeit with more order.

Despite this, the capacitance at zero charge is (in this theory) still fixed by the screening length ℓ, which means the underscreening paradox remains.[45] Further development of the presented theory, such as through taking into account the spatial structure of clusters/gel or accounting for electrostatics beyond that investigated here,[30] could help gain further insight into these puzzling experiments.

B. Overscreening

Ma *et al.*[51] performed sophisticated classical density functional calculations of a coarse-grained IL with varying degrees of ion pairing, up to that suggested by Gebbie *et al.*[36] It was noted that the charged density was somewhat insensitive to the extent of ion pairing, which suggested a link between ion pairing and overscreening. This was further shown by Avni *et al.*,[58] where a link between clusters (ion pairs, triplets and quadruplets) and the linearized overscreening theory of Bazant–Storey–Kornyshev (BSK)[28] occurs in the long-wavelength limit. However, the BSK theory is known to underestimate overscreening in ILs and the interpretation of it can be subtle,[87–89] with some suggesting that short-range cation–anion repulsion occurs. The alternating "copolymer" structure of the gel/large clusters is conceptually similar to extended overscreening structures (bulk or in the EDL). If one accounts for the spatial structure of larger clusters (than ion pairs, triplets and quadruplets[58]) or the gel, extended overscreening could potentially be obtained.

Here, for large association constants, we found that the EDL structure has two regimes: one where electrode charge is screened by free ions and another where it is screened by the gel. The free ions accumulate near the interface, with the gel persisting toward the bulk. Conceptually, this could be considered similar to the overscreening–crowding transition.[28]

The reader should also bear in mind that the EDL theory presented here is a simple, local density approximation, which cannot explicitly account for overscreening or the internal charge distribution of clusters. However, while a spatial map between ions in clusters, assumed to be Cayley trees here, and charge density does not yet exist, Cayley trees have well-defined shells around an ion in a cluster. One can loosely interpret the number of shells around an ion with the distance from that ion, which can be utilized to further establish the link between associations and overscreening.

Let us consider a cation at a "central" lattice site and examine the probability of an anion being at any of the lattice sites n shells away from the central cation, similar to the pair correlation function between cations and anions. The anion can be present on that lattice site either by being linked to the central cation as part of the same cluster, p, or by random, p_-^r. There is also a possibility that a cation could be present on that site by random, p_+^r. Assuming that unassociated species are uncorrelated, $p_-^r = p_+^r = p^r$, and taking into account the incompressibility condition, we obtain $p^r = (1 - p)/2$.

Thus, the total probability of observing an anion one shell away is $(1 + p)/2$. For the next shell, the probability that an anion is there via a link to the central cation is exactly zero, as we require alternating associations. However, there is some probability that an anion (or cation) is there by chance. In this case, the random probability of an anion is $(1 - p^2)/2$, which is in fact the total probability of seeing an anion two shells away. Similarly, the analysis for three shells away yields an anion probability of $(1 + p^3)/2$. Thus, we can generalize the probability of seeing an anion n shells away from a central cation to

$$\mathcal{P}_{+-} = \frac{1 + p^n(-1)^{n+1}}{2}. \tag{26}$$

In Fig. 13, $\mathcal{P}_{+-}$ is plotted as a function of n, where we see that the correlation probabilities display pronounced overscreening when $\lambda = 10$, but only modest overscreening for $\lambda = 1$. Therefore, pronounced overscreening could be more consistent with the gel than clusters. While the developed theory does not spatially resolve the clusters/gel, further development for the spatial distribution of ions in clusters/gel could shed light on this connection.

In this spirit, one issue of the theory (which presumably needs to be dealt with before this can be achieved) is how can extremely large clusters screen the field if the latter decays on a significantly shorter length scale than the clusters? This is a well-known issue for theories of ILs with simple, local density approximations when no associations are included. Taking into account associations increases the screening length relative to the Debye length, but the clusters can become extremely large in size. Therefore, the issue can remain for finite clusters, and perhaps a finite cutoff needs to be introduced for clusters which can contribute to the screening of electrode charge, as is the case of the conductivity of ions in ILs.[49,79] For the gel, it is conceptually reasonable to think of its composition as locally changing, just as an iceberg melts from its surface. For clusters, their individual structures cannot locally vary as they are discrete. In any case, the theory should work for a large number of free ions and a small number of free ions, and it should act as an interpolation scheme between these two regimes, with the largest error occurring only right at the gel point (where there are significant numbers of very large clusters).

In addition to the above issue is the applicability of a local density approximation when there are substantial variations of the
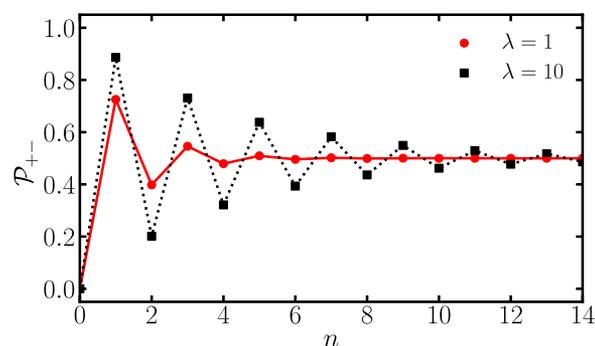

FIG. 13. Pronounced overscreening could occur as a result of the associations between ions. The probability of an anion n shells away from a central cation. The functionality was taken to be 3.

charge density on a smaller length scale than the screening length, i.e., the fact there is internal structure to the clusters. The presented theory cannot capture these short-scale variations, with it only being able to deal with mean-field volume fractions of clusters of different ranks and the gel. By developing theories that more accurately account for spatial correlations from electrostatics and non-electrostatic interactions, and that also account for the internal structures of clusters, the overscreening structures and screening lengths observed in surface force experiments could, perhaps, be more accurately described.

C. Assumptions of the theory

The developed theory has some shortcomings, as just described, but how well do we expect it to handle the averaged volume fractions of each cluster? There could potentially be a number of issues with the developed theory at a charged interface that could cause it to break down. Some examples are as follows:

1. Do Cayley tree clusters exist near an interface?
2. Do specific interactions with the interface cause formation of the compact layer?
3. Do ion pairs and aggregates rotate in the electrostatic fields?
4. Does the association free energy depend on the electrostatic field?

For each of these questions, we shall state what is expected to happen and how to confirm/falsify these expectations. Point 1 is the major question to be answered, with the remaining points being minor if 1 is found to hold reasonably. In the description of 1, some details of how to test the cluster distribution shall also be given. Overall, it is expected that the cluster distribution in the EDL does not exactly hold, but we believe it is a sufficiently good approximation to understand the qualitative behavior.

1. Cayley trees and cluster distribution in the EDL

We have shown that clusters are destroyed in favor of free ions at large electrostatic potentials; therefore, the assumption of Cayley tree clusters is not important at large fields. What needs to be tested, however, is the low-voltage regime of overscreening. Close to the interface, the presence of the interface could block association sites of the ions and drive the ions to form intra-cluster loops. The assumption of Cayley trees applying in the EDL and the assumed cluster distribution can only be confirmed from molecular simulations.

In bulk ILs, McEldrew et al.[49] found that the spatial distribution function (SDF) of cations (anions) around anions (cations) has well-defined "hot spots" (for where the concentration is over twice the bulk value), where the ions of opposite sign prefer to reside. When the cations and anions reside in each other's hot spots, an association was defined.[49] This highly directional interaction between cations and anions is a consequence of the complicated shapes of the ions in ILs, and it is fundamental to the formation of Cayley tree clusters,[77] Spherical cutoffs to define associations or kinetic criteria[62] are not sufficient to test this approximation. Moreover, Lennard-Jones hard sphere approximation to coarse-graining cannot be used, as the full atomistic details are required to capture these complex interactions. To see if Cayley tree clusters hold in the EDL, the association

criteria of McEldrew et al.[49] must be utilized to calculate the clusters in the EDL. This cluster distribution can be compared against the presented theory to test how well the assumed cluster distribution holds. Note that in the simulations, to obtain the volume fraction of each cluster, the clusters will have to be assigned to bins. The size of these bins should be larger than the average size of clusters, which might become problematic right near the gel point when the cluster sizes become very large.

The gel will also be evident from using the association criteria of McEldrew et al.[49] as a percolating ionic network throughout the simulation. The theory predicts that the gel continuously exists, but it changes composition as a function of the interface. Inspection of the percolating ionic network should be able to reveal if there is an equivalence between overscreening and gel screening. It would also be interesting to test the connection between the associations and overscreening in the bulk.

2. Specific interactions with the interface

The ions can interact with the interface "specifically" through non-electrostatic interactions, which often causes one type of ion to accumulate at the interface without an applied voltage, owing to the specific interaction of one type of ion being more favorable than the other. These specific interactions with the surface are not accounted for in the presented theory, and they will further contribute to breaking the assumed cluster distribution. Therefore, the presented theory might only work well for the diffuse part of the double layer, not the compact layer of ions that are in contact with the interface.

In a similar spirit to the presented theory, several theories to describe the voltage dependence of the compact layer with clusters were developed by Damaskin–Frumkin–Parsons.[90,91] In those theories, the equilibrium between the free states and clustered states were self-consistently determined in an electrostatic potential, which gave rise to a voltage dependence of the differential capacitance of the compact layer. To account for specific interactions with the interface, one approach could be to have an additional equilibrium between the compact layer, described by the theories of Damaskin–Frumkin–Parsons,[90,91] and the diffuse part of the EDL.

Again, molecular dynamics simulations can be utilized to test if specific interactions cause a breakdown of the cluster distribution, using the cluster criteria of McEldrew et al.[49]

3. Orientation of clusters

As overscreening is a spatially ordered structure, it is expected that clusters do orient in an electrostatic field. However, we do not expect them to behave as fluctuating Langevin dipoles. It has been shown in Refs. 49 and 53 that the lifetime of associations is of the order of ~1–10 ps, which is presumably too short for the rotation of an ion pair or cluster. Therefore, the orientation of clusters must be a weaker contribution than fluctuating Langevin dipoles. In Ref. 92, ion pairs (which were not permitted to dissociate in the EDL) were treated as Langevin dipoles, where an additional bump in concentrations of ion pairs and a higher propensity for a "bell"-shaped differential capacitance curve because of dielectric saturation were found. While ion pairs might not behave as fluctuating Langevin dipoles, the large clusters and gel could have vibrational modes that contribute to the dielectric screening of the electrolyte. This could be introduced in a similar way to Ref. 92, as some effective dielectric

constant that is saturated to lower values in the crowding regime. Thus, it is expected that this issue is not substantial for the averaged volume fractions, but it could cause a breakdown of the assumed cluster distribution, as outlined in the supplementary material. The issue of orientation of clusters can again be confirmed by molecular simulations, provided the cluster distribution can be calculated as described in the previous point.

4. Field dependent binding

Related to the previous points, if an ion pair is oriented along the decay of the electrostatic field, the ion pair will presumably be stretched. This could be captured through an electrostatic field-dependent binding energy and, therefore, association constant. We would expect the binding energy to decrease with increasing electrostatic fields. This will cause the associations to break down more than shown here. The presented theory could be considered to overestimate the extent of clusters in the EDL, then. Again, this issue can be confirmed from computing the cluster distribution in the EDL and comparing it against the presented theory.

VII. CONCLUSION

In summary, we have developed a theory for the EDL in ILs that accounts for thermoreversible associations, based on that of McEldrew *et al.* in bulk ILs. The developed theory is constructed from assuming that the bulk cluster distribution applies in the EDL, but with modulated volume fractions of cations and anions, which is coupled to the Poisson equation through a Boltzmann closure relation of the free ions. This theory was shown to recover the expected linear response behavior and the large potential limits. Therefore, it should serve as a qualitative description for the EDL of an IL with thermoreversible associations. For strongly associating ILs, the free ions crowd near the interface; but far from the interface, the gel screens the electrode charge. The differential capacitance was found to have a larger capacitance at zero charge than free ion theories, from the fact that the clusters can also screen, and the transition to "camel" shape occurs at smaller free ion fractions than models based on free ions.

ILs provided an extremely useful test ground to develop the theory presented here, since ILs are the simplest possible superconcentrated electrolytes. It is expected that the presented theory can describe coarse-grained values of the volume fractions of each cluster in the EDL of ILs previously studied by McEldrew *et al.*, and other similar ILs from the combinations of the different cations and anions studied therein. The aggregation and gelation theory of McEldrew *et al.* has also been developed for water-in-salt electrolytes and salt-in-ionic liquids, so far. Development of the EDL theory for these systems would be relevant for engineering the interfacial behavior of such electrolytes, which is crucial for their performance in energy storage technologies. Moreover, investigating the consequences of this theory for the electrokinetic behavior could potentially yield new predictions to confirm the presented theory.

SUPPLEMENTARY MATERIAL

In the supplementary material, further details of the bulk cluster distribution are given, the bulk–electrical double layer equilibrium is established and the approximations required are outlined, the role of gel terms in the closure relation is outlined, and finally a step-by-step guide of how to implement the equations numerically is given.

NOMENCLATURE

List of variables and parameters. Top panel—quantities used for the cluster distribution. A * is used to denote values at the gel point. Bottom panel—quantities used in the EDL. A bar is used over any of the variables in the top panel if they are in the EDL.

Top panel

N_{lm}	Number of lm clusters
N_i^{gel}	Number of species i in gel
f_i	Functionality of species i
v_i	Volume of species i
Ω	Number of lattice sites
β	Inverse thermal energy
c_{lm}	Concentration of cluster (number per lattice site)
ϕ_{lm}	Volume fraction of an lm cluster
ϕ_i	Total volume fraction of species i
c_i^{gel}	Concentration of species i in gel
ϕ_i^{sol}	Volume fraction of species i in sol
ϕ_i^{gel}	Volume fraction of species i in gel
w_i^{sol}	Fraction of species in the sol
w_i^{gel}	Fraction of species in the gel
Δ_{lm}	Free energy of formation of a cluster of a rank lm
Δ_i^{gel}	Free energy change of species i associating to the gel
Δf_{+-}	Free energy of an association
W_{lm}	Combinatorial enumeration
Δu_{+-}	Association energy
Δs_{+-}	Entropy of an association
λ	Association constant
ζ	Number of anion–cation associations
p_{ij}	Association probabilities
p_{ij}^{sol}	Association probabilities in the sol

Bottom panel

u	Volts in units of thermal voltage
α	Short-range correlation parameter
κ	Inverse Debye length

ℓ	Screening length
e	Elementary charge
$\epsilon\epsilon_0$	Dielectric constant
$\delta\tilde{\phi}$	Perturbation in volume fractions
$\delta\tilde{p}$	Perturbation in probabilities
$\delta\tilde{\phi}^{sol}$	Perturbation in sol volume fractions
$\delta\tilde{p}^{sol}$	Perturbation in sol probabilities
C	Differential capacitance
C_0	Debye capacitance
$\tilde{\sigma}$	Dimensionless surface charge density
u_0	Potential drop across EDL

AUTHOR DECLARATIONS

Conflict of Interest

The authors have no conflicts to disclose.

Author Contributions

Zachary A. H. Goodwin: Conceptualization (equal); Data curation (lead); Formal analysis (lead); Investigation (lead); Methodology (lead); Software (equal); Writing – original draft (lead); Writing – review & editing (lead). **Michael McEldrew**: Conceptualization (equal); Investigation (equal); Methodology (equal); Software (equal); Writing – review & editing (equal). **J. Pedro de Souza**: Investigation (equal); Methodology (equal); Software (equal); Writing – review & editing (equal). **Martin Z. Bazant**: Funding acquisition (equal); Resources (equal); Supervision (equal); Writing – review & editing (equal). **Alexei A. Kornyshev**: Funding acquisition (equal); Resources (equal); Supervision (equal); Writing – review & editing (equal).

DATA AVAILABILITY

The data that support the findings of this study are available from the corresponding author upon reasonable request.

REFERENCES

[1] T. Welton, Chem. Rev. **99**, 2071 (1999).

[2] J. P. Hallett and T. Welton, Chem. Rev. **111**, 3508 (2011).

[3] M. V. Fedorov and A. A. Kornyshev, Chem. Rev. **114**, 2978 (2014).

[4] H. Weingärtner, Angew. Chem., Int. Ed. **47**, 654 (2008).

[5] S. Kondrat and A. A. Kornyshev, Nanoscale Horiz. **1**, 45 (2016).

[6] C. Y. Son and Z.-G. Wang, J. Chem. Phys. **153**, 100903 (2020).

[7] L. Suo, O. Borodin, T. Gao, M. Olguin, J. Ho, X. Fan, C. Luo, C. Wang, and K. Xu, Science **350**, 938 (2015).

[8] L. Suo, O. Borodin, Y. Wang, X. Rong, W. Sun, X. Fan, S. Xu, M. A. Schroeder, A. V. Cresce, F. Wang *et al.*, Adv. Energy Mater. **7**, 1701189 (2017).

[9] J. Vatamanu and O. Borodin, J. Phys. Chem. Lett. **8**, 4362 (2017).

[10] P. Lannelongue, R. Bouchal, E. Mourad, C. Bodin, M. Olarte, S. le Vot, F. Favier, and O. Fontaine, J. Electrochem. Soc. **165**, A657 (2018).

[11] M. Chen, G. Feng, and R. Qiao, Curr. Opin. Colloid Interface Sci. **47**, 99 (2020).

[12] M. McEldrew, Z. A. H. Goodwin, A. A. Kornyshev, and M. Z. Bazant, J. Phys. Chem. Lett. **9**, 5840 (2018).

[13] M. Han, R. Zhang, A. A. Gewirth, and R. M. Espinosa-Marzal, Nano Lett. **21**, 2304 (2021).

[14] T. S. Groves, C. S. Perez-Martinez, R. Lhermerout, and S. Perkin, J. Phys. Chem. Lett. **12**, 1702 (2021).

[15] O. Patsahan and A. Ciach, ACS Omega **7**, 6655 (2022).

[16] Z. Yu, N. P. Balsara, O. Borodin, A. A. Gewirth, N. T. Hahn, E. J. Maginn, K. A. Persson, V. Srinivasan, M. F. Toney, K. Xu, K. R. Zavadil, L. A. Curtiss, and L. Cheng, ACS Energy Lett. **7**, 461 (2022).

[17] R. Zhang, M. Han, K. Ta, K. E. Madsen, X. Chen, X. Zhang, R. M. Espinosa-Marzal, and A. A. Gewirth, ACS Appl. Energy Mater. **3**, 8086 (2020).

[18] K. Dokko, N. Tachikawa, K. Yamauchi, M. Tsuchiya, A. Yamazaki, E. Takashima, J.-W. Park, K. Ueno, S. Seki, N. Serizawa *et al.*, J. Electrochem. Soc. **160**, A1304 (2013).

[19] A. Lewandowski and A. Świderska-Mocek, J. Power Sources **194**, 601 (2009).

[20] N. Molinari, J. P. Mailoa, and B. Kozinsky, J. Phys. Chem. Lett. **10**, 2313 (2019).

[21] N. Molinari, J. P. Mailoa, N. Craig, J. Christensen, and B. Kozinsky, J. Power Sources **428**, 27 (2019).

[22] Y. Zhang, R. Ye, D. Henkensmeier, R. Hempelmann, and R. Chen, Electrochim. Acta **263**, 47 (2018).

[23] H. Yoon, P. C. Howlett, A. S. Best, M. Forsyth, and D. R. Macfarlane, J. Electrochem. Soc. **160**, A1629 (2013).

[24] P. C. Howlett, D. R. MacFarlane, and A. F. Hollenkamp, Electrochem. Solid-State Lett. **7**, A97 (2004).

[25] M. V. Fedorov and A. A. Kornyshev, J. Phys. Chem. B **112**, 11868 (2008).

[26] M. V. Fedorov and A. A. Kornyshev, Electrochim. Acta **53**, 6835 (2008).

[27] N. Georgi, A. A. Kornyshev, and M. V. Fedorov, J. Electroanal. Chem. **649**, 261 (2010).

[28] M. Z. Bazant, B. D. Storey, and A. A. Kornyshev, Phys. Rev. Lett. **106**, 046102 (2011).

[29] S. W. Coles, C. Park, R. Nikam, M. Kanduč, J. Dzubiella, and B. Rotenberg, J. Phys. Chem. B **124**, 1778 (2020).

[30] J. P. de Souza, Z. A. H. Goodwin, M. McEldrew, A. A. Kornyshev, and M. Z. Bazant, Phys. Rev. Lett. **125**, 116001 (2020).

[31] J. P. de Souza, K. Pivnic, M. Z. Bazant, M. Urbakh, and A. A. Kornyshev, J. Phys. Chem. B **126**, 1242 (2021).

[32] N. Gavish, D. Elad, and A. Yochelis, J. Phys. Chem. Lett. **9**, 36 (2018).

[33] E. Krucker-Velasquez and J. W. Swan, J. Chem. Phys. **155**, 134903 (2021).

[34] A. Levy, M. McEldrew, and M. Z. Bazant, Phys. Rev. Mater. **3**, 055606 (2019).

[35] A. M. Smith, A. A. Lee, and S. Perkin, J. Phys. Chem. Lett. **7**, 2157 (2016).

[36] M. A. Gebbie, M. Valtiner, X. Banquy, E. T. Fox, W. A. Henderson, and J. N. Israelachvili, Proc. Natl. Acad. Sci. U. S. A. **110**, 9674 (2013).

[37] M. A. Gebbie, H. A. Dobbs, M. Valtiner, and J. N. Israelachvili, Proc. Natl. Acad. Sci. U. S. A. **112**, 7432 (2015).

[38] M. A. Gebbie, A. M. Smith, H. A. Dobbs, A. A. Lee, G. G. Warr, X. Banquy, M. Valtiner, M. W. Rutland, J. N. Israelachvili, S. Perkin, and R. Atkin, Chem. Commun. **53**, 1214 (2017).

[39] A. M. Smith, A. A. Lee, and S. Perkin, Phys. Rev. Lett. **118**, 096002 (2017).

[40] M. Han, H. Kim, C. Leal, M. Negrito, J. D. Batteas, and R. M. Espinosa-Marzal, Adv. Mater. **7**, 2001313 (2020).

[41] L. A. Jurado, H. Kim, A. Rossi, A. Arcifa, J. K. Schuh, N. D. Spencer, C. Leal, R. H. Ewoldt, and R. M. Espinosa-Marzal, Phys. Chem. Chem. Phys. **18**, 22719 (2016).

[42] L. A. Jurado, H. Kim, A. Arcifa, A. Rossi, C. Leal, N. D. Spencer, and R. M. Espinosa-Marzal, Phys. Chem. Chem. Phys. **17**, 13613 (2015).

[43] L. A. Jurado and R. M. Espinosa-Marzal, Sci. Rep. **7**, 4225 (2017).

[44] X. Mao, P. Brown, C. Červinka, G. Hazell, H. Li, Y. Ren, D. Chen, R. Atkin, J. Eastoe, I. Grillo, A. A. H. Padua, M. F. C. Gomes, and T. A. Hatton, Nat. Mater. **18**, 1350 (2019).

[45] A. A. Lee, C. S. Perez-Martinez, A. M. Smith, and S. Perkin, Faraday Discuss. **199**, 239 (2017).

[46] A. A. Lee, C. S. Perez-Martinez, A. M. Smith, and S. Perkin, Phys. Rev. Lett. **119**, 026002 (2017).

[47] Y. Wang and G. A. Voth, J. Am. Chem. Soc. **127**, 12192 (2005).

[48] C. E. S. Bernardes, M. E. M. da Piedade, and J. N. C. Lopes, J. Phys. Chem. B **115**, 2067 (2011).

[49] M. McEldrew, Z. A. H. Goodwin, H. Zhao, M. Z. Bazant, and A. A. Kornyshev, J. Phys. Chem. B **125**, 2677 (2021).

[50] J. N. A. C. Lopes and A. A. H. Pádua, J. Phys. Chem. B **110**, 3330 (2006).

[51] K. Ma, J. Forsman, and C. E. Woodward, J. Chem. Phys. **142**, 174704 (2015).

[52] A. A. Lee, D. Vella, S. Perkin, and A. Goriely, J. Phys. Chem. Lett. **6**, 159 (2015).

[53] Y. Zhang and E. J. Maginn, J. Phys. Chem. Lett. **6**, 700 (2015).

[54] D. R. MacFarlane, M. Forsyth, E. I. Izgorodina, A. P. Abbott, G. Annat, and K. Fraser, Phys. Chem. Chem. Phys. **11**, 4962 (2009).

[55] O. Hollóczki, F. Malberg, T. Welton, and B. Kirchner, Phys. Chem. Chem. Phys. **16**, 16880 (2014).

[56] R. M. Adar, T. Markovich, and D. Andelman, J. Chem. Phys. **146**, 194904 (2017).

[57] J. C. Araque, S. K. Yadav, M. Shadeck, M. Maroncelli, and C. J. Margulis, J. Phys. Chem. B **119**, 7015 (2015).

[58] Y. Avni, R. M. Adar, and D. Andelman, Phys. Rev. E **101**, 010601 (2020).

[59] Z. A. H. Goodwin, G. Feng, and A. A. Kornyshev, Electrochim. Acta **225**, 190 (2017).

[60] M. Chen, Z. A. H. Goodwin, G. Feng, and A. A. Kornyshev, J. Electroanal. Chem. **819**, 347 (2018).

[61] Z. A. H. Goodwin and A. A. Kornyshev, Electrochem. Commun. **82**, 129 (2017).

[62] G. Feng, M. Chen, S. Bi, Z. A. Goodwin, E. B. Postnikov, N. Brilliantov, M. Urbakh, and A. A. Kornyshev, Phys. Rev. X **9**, 021024 (2019).

[63] J. Dupont, J. Braz. Chem. Soc. **15**, 341 (2004).

[64] M. McEldrew, Z. A. H. Goodwin, S. Bi, M. Z. Bazant, and A. A. Kornyshev, J. Chem. Phys. **152**, 234506 (2020).

[65] M. McEldrew, Z. A. H. Goodwin, S. Bi, A. A. Kornyshev, and M. Z. Bazant, J. Electrochem. Soc. **168**, 050514 (2021).

[66] M. McEldrew, Z. A. H. Goodwin, N. Molinari, B. Kozinsky, A. A. Kornyshev, and M. Z. Bazant, J. Phys. Chem. B **125**, 13752 (2021).

[67] P. J. Flory, J. Chem. Phys. **10**, 51 (1942).

[68] F. Tanaka, Macromolecules **22**, 1988 (1989).

[69] F. Tanaka, Macromolecules **23**, 3784 (1990).

[70] F. Tanaka and W. H. Stockmayer, Macromolecules **27**, 3943 (1994).

[71] F. Tanaka and M. Ishida, J. Chem. Soc. Faraday Trans. **91**, 2663 (1995).

[72] M. Ishida and F. Tanaka, Macromolecules **30**, 3900 (1997).

[73] F. Tanaka, Physica A **257**, 245 (1998).

[74] F. Tanaka and M. Ishida, Macromolecules **32**, 1271 (1999).

[75] F. Tanaka, Polym. J. **34**, 479 (2002).

[76] O. Borodin, L. Suo, M. Gobet, X. Ren, F. Wang, A. Faraone, J. Peng, M. Olguin, M. Schroeder, M. S. Ding *et al.*, ACS Nano **11**, 10462 (2017).

[77] J.-H. Choi, H. Lee, H. R. Choi, and M. Cho, Annu. Rev. Phys. Chem. **69**, 125 (2018).

[78] J. Jeon, H. Lee, J.-H. Choi, and M. Cho, J. Phys. Chem. C **124**, 11790 (2020).

[79] A. France-Lanord and J. C. Grossman, Phys. Rev. Lett. **122**, 136001 (2019).

[80] Z. A. H. Goodwin, J. P. de Souza, M. Z. Bazant, and A. A. Kornyshev, "Mean-field theory of the electrical double layer in ionic liquids," in *Encyclopedia of Ionic Liquids*, edited by S. Zhang (Springer, Singapore, 2021).

[81] A. A. Kornyshev, J. Phys. Chem. B **111**, 5545 (2007).

[82] M. S. Kilic, M. Z. Bazant, and A. Ajdari, Phys. Rev. E **75**, 021502 (2007).

[83] M. Z. Bazant, M. S. Kilic, B. D. Storey, and A. Ajdari, Adv. Colloid Interface Sci. **152**, 48 (2009).

[84] A. A. Kornyshev and M. A. Vorotyntsev, Electrochim. Acta **26**, 303 (1981).

[85] Y. A. Budkov, A. L. Kolesnikov, Z. A. H. Goodwin, M. G. Kiselev, and A. A. Kornyshev, Electrochim. Acta **284**, 346 (2018).

[86] M. Jitvisate and J. R. T. Seddon, J. Phys. Chem. Lett. **9**, 126 (2018).

[87] J. P. de Souza and M. Z. Bazant, J. Phys. Chem. C **124**, 11414 (2020).

[88] H. Chao and Z.-G. Wang, J. Phys. Chem. Lett. **11**, 1767 (2020).

[89] A. A. Lee, S. Kondrat, D. Vella, and A. Goriely, Phys. Rev. Lett. **115**, 106101 (2015).

[90] B. B. Damaskin and A. N. Frumkin, Electrochim. Acta **19**, 173 (1974).

[91] R. Parsons, J. Electroanal. Chem. Interfacial Electrochem. **59**, 229 (1975).

[92] Y. Zhang, T. Ye, M. Chen, Z. A. H. Goodwin, G. Feng, J. Huang, and A. A. Kornyshev, Energy Environ. Mater. **3**, 414 (2020).